Remote Sensing of Environment 201 (2017) 73–87

Contents lists available at ScienceDirect

Remote Sensing of Environment

journal homepage: www.elsevier.com/locate/rse

Annual dynamics of forest areas in South America during 2007–2010 at 50-m spatial resolution

Yuanwei Qin[a], Xiangming Xiao[a,b,*], Jinwei Dong[a,c], Yuting Zhou[a], Jie Wang[a], Russell B. Doughty[a], Ying Chen[d], Zhenhua Zou[a], Berrien Moore III[e]

[a] Department of Microbiology and Plant Biology, Center for Spatial Analysis, University of Oklahoma, Norman, OK 73019, USA
[b] Ministry of Education Key Laboratory of Biodiversity Science and Ecological Engineering, Institute of Biodiversity Science, Fudan University, Shanghai, 200433, China
[c] Institute of Geographical Science and Natural Resource Research, Chinese Academy of Sciences, Beijing 100101, China
[d] Fujian Agriculture and Forestry University, Fuzhou, Fujian 350002, China
[e] College of Atmospheric and Geographic Sciences, University of Oklahoma, Norman, OK, 73019, USA

ARTICLE INFO

Keywords:
Tropical forest
ALOS PALSAR
Forest map comparison
User community
Biodiversity conservation
Leaf area index
Forest definition

ABSTRACT

South America has the largest tropical rainforests and the richest biodiversity in the world. It is challenging to map tropical forests and their spatio-temporal changes because forests are facing fragmentation from human activities (e.g., logging, deforestation), drought, and fire, as well as persistent clouds. Here we present a robust approach to map forests in South America during 2007–2010 and analyze the consistency and uncertainty among eight major forest maps in South America. Greenness-relevant MOD13Q1 NDVI and structure/biomass-relevant ALOS PALSAR time series data recorded 2007 through 2010 were coupled to identify and map forests at 50-m spatial resolution. Both area and spatial comparison were conducted to analyze the consistency and uncertainty of these eight forest maps. Annual 50-m PALSAR/MODIS forest maps were generated during 2007–2010 and the total forest area in South America was about 8.63×10^6 km^2 in 2010. Large differences in total forest area (8.2×10^6 km^2–12.7×10^6 km^2) existed among these forest products, especially in the forest edges, semi-humid tropical, and subtropical regions. Forest products generated under a similar forest definition had similar or even larger variation than those generated with contrasting forest definitions. We also find out that one needs to consider leaf area index as an adjusting factor and use much higher threshold values in the Vegetation Continuous Field (VCF) datasets to estimate forest cover areas. Analyses of PALSAR/MODIS forest maps in 2008/2009 showed a relatively small rate of loss (3.2×10^4 km^2 year^{-1}) in net forest cover, similar to that of FAO FRA (3.3×10^4 km^2 year^{-1}), but much higher annual rates of forest loss and gain. The rate of forest loss (0.195×10^6 km^2 year^{-1}) was higher than that of Global Forest Watch (0.081×10^6 km^2 year^{-1}). PALSAR/MODIS forest maps showed that more deforestation occurred in the unfragmented forest areas. Caution should be used when using the different forest maps to analyze forest loss and make policies regarding forest ecosystem services and biodiversity conservation. The integration of PALSAR and MODIS images during 2007–2010 provides annual maps of forests in South America with improved accuracy and reduced uncertainty.

1. Introduction

Tropical forests are a huge reservoir of terrestrial carbon and estimated to hold 230–260 Pg C, or about 40–60% of the carbon contained in the world's terrestrial vegetation (Baccini et al., 2012; Pan et al., 2011; Saatchi et al., 2011; Zarin et al., 2016). Tropical forests are susceptible to multiple disturbances from logging (Fraser, 2014; Matricardi et al., 2013), expansion of industrial forest plantations and agricultural land (le Maire et al., 2014; Morton et al., 2006), drought (Brando et al., 2014), and fires (Fanin and van der Werf, 2015). Therefore, it is important for the scientific community to design and implement operational forest monitoring, reporting, and verification (MRV) systems that are reproducible, consistent, and accurate at national and continental scales, which is also a requirement of a successful REDD+ (Reduce Emissions from Deforestation and Forest Degradation) mechanism under the United Nations Framework Convention on Climate Change (UNFCCC). There is an urgent need for high accuracy forest maps so that land managers, policy makers, and scientists can investigate the changes in carbon fluxes, carbon stock, and ecological services, such as the degradation in the carbon stocks near tropical

* Corresponding author at: Department of Microbiology and Plant Biology, Center for Spatial Analysis, University of Oklahoma, Norman, OK 73019, USA
E-mail address: xiangming.xiao@ou.edu (X. Xiao).

http://dx.doi.org/10.1016/j.rse.2017.09.005
Received 10 March 2017; Received in revised form 26 August 2017; Accepted 2 September 2017
0034-4257/

forest edges (Chaplin-Kramer et al., 2015), habitat fragmentation (Haddad et al., 2015), and the effects of conservation policy on forest recovery (Viña et al., 2016).

Spaceborne remote sensing technology has the advantage of observing large areas of Earth's landscape at high temporal resolution with frequent revisits, and therefore is widely used for global and continental forest mapping. Optical remote sensing images, which have been collected since the 1970s, are the major data source for forest mapping because they are relatively easy to process and interpret. The optical sensor-based forest products are mainly produced based upon the 1000-m Advanced Very High Resolution Radiometer (AVHRR) (Achard et al., 2001), 500-m and 250-m Moderate Resolution Imaging Spectroradiometer (MODIS) (Friedl et al., 2010; Hansen et al., 2003; Townshend et al., 2011), and 30-m Landsat (Hansen et al., 2013; Kim et al., 2014). Selective logging is common in tropical forests and cannot be observed by relatively coarse spatial resolution images, especially for AVHRR and MODIS images (Asner et al., 2005). Active microwave remote sensing images are becoming more applicable to tropical forest mapping, especially as wall-to-wall global observations become available, such as C-band Sentinel-1, L-band Japanese Earth Resource Satellite 1 (JERS-1), and Advanced Land Observing Satellite (ALOS) Phased Array type L-band Synthetic Aperture Radar (PALSAR). Active microwave sensors can penetrate clouds and smoke haze, and monitor land surface conditions day and night without interference from weather conditions. The short wavelength X- and C-band SAR have been applied to forest mapping (Ranson and Sun, 1997), although these bands are easily saturated at the forest canopy. The L-band ALOS PALSAR has a long operating wavelength (23.6 cm), which is sensitive to forest structure and biomass under the canopy and is well suited to tropical forest monitoring. PALSAR imagery has also been successfully applied for global and regional forest mapping (Dong et al., 2012; Qin et al., 2016; Shimada et al., 2014).

Mapping tropical forests with high accuracy, either from optical or active microwave remote sensing, is very challenging. Tropical forest loss and recovery is occurring at high rates. For example, Brazil experienced a decreasing trend in forest cover from 2000 to 2012, with the annual average rate about $3 \times 10^4\,km^2\,year^{-1}$ (Hansen et al., 2013). Conversely, the industrial forest plantations are expanding due to the increased demand for pulp and wood, such as Eucalypt. The Eucalypt plantations have a short clear-cut and afforestation rotation in Brazil (le Maire et al., 2014). Time series remote sensing images are preferred for tracking these fast changes in forest cover. The availability of data from optical remote sensing is largely restricted by persistent clouds, which is the major barrier to tropical forest mapping (Achard et al., 2007; Asner, 2001). Many recent studies have generated forest cover maps by combining the increasing number of good quality optical remote sensing images from multiple years (European Space Agency, 2016; Hansen et al., 2013). However, the use of images from multiple-year periods might not detect intra-annual changes of forest cover in the Amazon Basin. A recent study evaluated eight global forest cover maps and showed that relatively large uncertainty existed among current forest maps (Sexton et al., 2015), particularly in the tropical zone (hotspots). Most of these forest maps are produced using image data from a single source. Single-data source based forest maps have moderate to large commission and omission errors because of complex landscapes. Different land cover types may have similar phenology and structural features, and the same land cover types may have different greenness attributes in different seasons.

Optical remote sensing can track the phenology of land cover types and active microwave remote sensing image can observe the structure and biomass of forests. There is a need to integrate active microwave and optical remote sensing imagery to map tropical forests (Dong et al., 2013; Qin et al., 2015; Reiche et al., 2016). Several studies have demonstrated the potential of combining SAR and optical remote sensing images for mapping land cover types (e.g., ice shelf change, urban areas, crops, and forests) (Ban, 2003; Khazendar et al., 2007; Qin et al., 2017; Ranson et al., 2003) and forest biomass (Lucas et al., 2006). The associated technical challenges of fusing microwave and optical remote sensing images for mapping changes in forest cover has also been addressed by several recent studies (Lehmann et al., 2015; Reiche et al., 2015). These studies have demonstrated a reduction in cloud–induced gaps in the observational data and improved accuracy in forest cover and forest cover change, even for areas with persistent cloud cover. However, these data fusion approaches were only demonstrated at a local scale and were not applied and tested for large-scale forest mapping in South America (Reiche et al., 2016).

In this study, we selected South America as the study area, which encompasses the Amazon Basin and contains the world's largest area of tropical rainforests and hosts the richest biodiversity (Malhi et al., 2008). South America had the highest forest loss rate with over 50% of tropical forest loss occurring since 2000 (Hansen et al., 2013). Both the forest loss rate and the net forest loss rate decreased after 2005, especially between 2010 and 2015 (Hansen et al., 2013; Keenan et al., 2015). The objectives of this study are three-fold. First, we produce annual maps of forest in South America at the spatial resolution of 50 m through the integration and analyses of PALSAR images (50-m spatial resolution) and time series MODIS NDVI images (250-m spatial resolution) during 2007–2010. This reflects (1) an improvement in terms of optical and microwave image data integration over a previous work in Southeast Asia that used only PALSAR images (Dong et al., 2012), and (2) an effort for expansion of the same mapping approach used in China (Qin et al., 2015) and monsoon Asia (Qin et al., 2016) towards global mapping of forests. Second, we compare and analyze the consistency and uncertainty among eight forest cover products for the year 2010, which were generated from various data sources and methods. Third, we quantify the spatio-temporal changes of forests in South America from 2008 to 2009, based on the resultant annual PALSAR/MODIS forest maps. This study provided improved forest cover maps for the user community of forests maps, which can be used for the development and application of forest management techniques in South America.

2. Materials and methods

We built a detailed workflow for forest cover mapping and forest cover product comparison in South America (Fig. 1). This workflow included two major components. First, we produced the annual 50-m PALSAR/MODIS forest maps from 2007 through 2010 based on the integration of PALSAR and MODIS NDVI data. Second, we analyzed the area and spatial differences in forest cover estimation from the PALSAR/MODIS forest cover map and seven other major forest cover products in 2010.

2.1. Study area

South America is mainly located from 56° S to 12° N, from 35° W to 81° W and covers an area of about 18 million square km^2. The elevation ranges from sea level to over 7000 m. South America can be divided into three major natural regions: the Andes Mountains, Eastern Highlands, and Plains. South America has humid tropical and semi-humid tropical climate in the north and humid subtropical climate in the southeast.

2.2. PALSAR data and pre-processing

The 50-m ALOS PALSAR Fine Beam Dual polarization (FBD) product from 2007 through 2010 were downloaded from the Earth Observation Research Center, Japan Aerospace Exploration Agency (JAXA). PALSAR HH and HV backscatter data are slope corrected and ortho-rectified with a geometric accuracy of about 12 m, and radiometrically calibrated. The Digital Number (DN) values (amplitude values) were converted into gamma-naught backscattering coefficients in decibels (γ°)

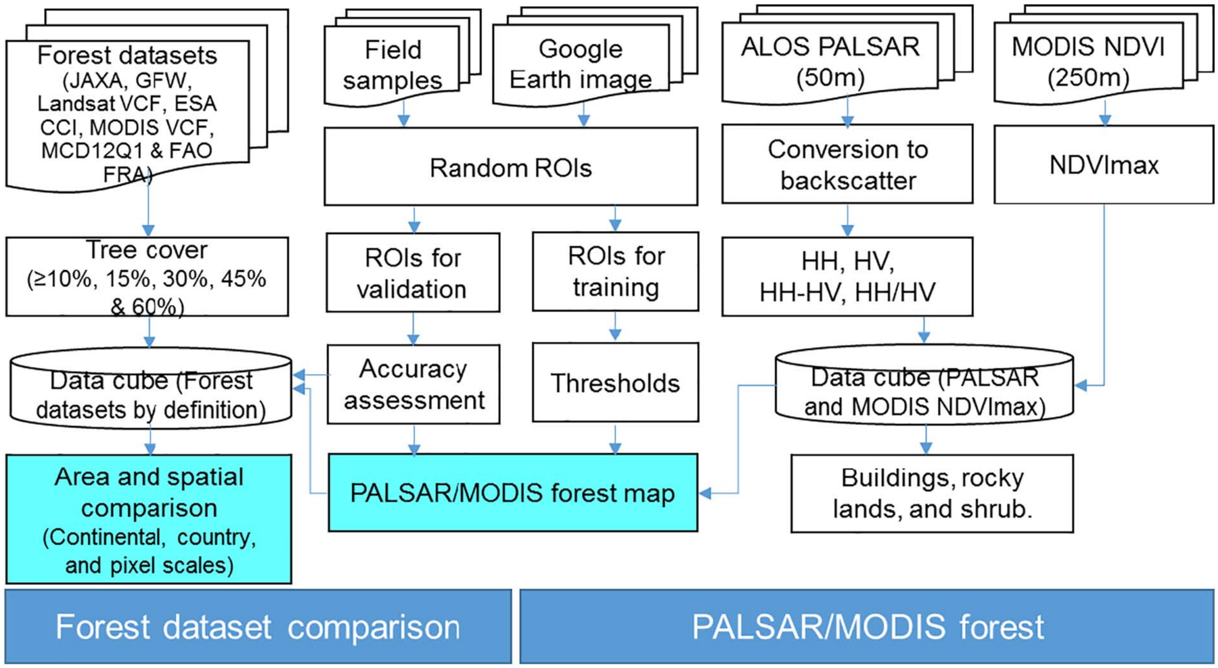

Fig. 1. The workflow of forest cover mapping and forest cover products comparison from multiple sources in South America.

using a calibration coefficient.

$$\gamma^{\circ} = 10 \times log_{10} < DN^2 > + CF \quad (1)$$

where CF is the absolute calibration factor of −83 (Shimada et al., 2009). PALSAR Difference and Ratio layers were calculated as:

$$Difference = HH - HV \quad (2)$$

$$Ratio = {}^{HH}\!/_{HV} \quad (3)$$

The visual interpretation of the false color composition of PALSAR HH, HV, and Difference (Fig. 2A) show their potential for mapping tropical forests from other land cover types, especially sparsely vegetated land.

2.3. MODIS NDVI data and pre-processing

MODIS/Terra MOD13Q1 product (Vegetation Indices 16-Day L3 Global 250 m) for South America from 2007 through 2010 was downloaded. The MOD13Q1 is a composite product with the best quality pixel in each 16-day window from daily observation. NDVI was calculated based on the red and near-infrared reflectance. The pixel quality and reliability layers in MOD13Q1 product were used to further exclude the poor-quality pixels in time series analysis. The number and ratio of good-quality observations from MOD13Q1 NDVI have high spatial difference in South America (Fig. 2B–C). About 52% of pixels had 15 (60%) or less good-quality observations annually and most of them were in the Amazon Basin. About 48% of pixels had 16 (60%) or more annual, good-quality observations in the southern portion of the study area. The 16-day NDVI layers for a year were used to calculate the annual maximum NDVI (NDVImax) values for each pixel from 2007 through 2010 (Fig. 2D).

2.4. PALSAR/MODIS forest mapping approach

According to the FAO, forest is defined as land with tree canopy cover > 10% and with a minimum tree height of five meters (Food and Agriculture Organization of the United Nations, 2012). The L-band ALOS PASLAR wavelengths have the capability to penetrate the tree canopy and interact with the tree trunks and branches. PALSAR data shows higher volume backscatter signals for forests than those of cropland, grassland, and water bodies. Therefore, PALSAR observations are sensitive to forest biomass and structure. Annual PALSAR HH and HV values are relatively stable from 2007 through 2010 in South America (Fig. 3A–B). The threshold values for the PALSAR-based forest mapping at 50-m spatial resolution were described in a previous study for monsoon Asia (Qin et al., 2016) and mainland Southeast Asia (Dong et al., 2012). Some land cover types, e.g., buildings, rocky land, and parts of bare land also have obvious structural features similar to forests and are easily confused with the PALSAR-based forests. Almost all the forest pixels with 10% or higher forest cover had NDVImax values equal to or larger than 0.5 and bare land dominated pixels had very low NDVImax values based on the relationship between visually interpreted Landsat-based land cover types and MOD13Q1 NDVImax in monsoon Asia (Qin et al., 2016). To reduce these commission errors for forest mapping, we combined PALSAR and MOD13Q1 NDVImax to generate annual maps of PALSAR/MODIS forests at 50-m spatial resolution in South America (Fig. 3C–D) using the thresholds: $-15 \le HV \le -9$, $3 \le Difference \le 7$, $0.35 \le Ratio \le 0.75$, and $NDVImax \ge 0.5$ (Qin et al., 2016).

We quantified the total area and mapped the spatial characteristics of forest cover change in South America from 2008 to 2009. First, we identified the forest/non-forest cover in individual years from 2007 through 2010 for each pixel using the proposed thresholds. Then we applied a three-year moving window filter to check temporal consistency in forest and non-forest over years. Out of the 4 year data, we have a total of 12 permutations (P(4,2) = 4!/(4−2)!) to reduce the uncertainty of forest change detection, which has been demonstrated in other land cover studies (Li et al., 2015; Yuan et al., 2005). This post-processing could not be applied to the forest maps in the first year (2007) and the last year (2010). Therefore, we reported forest change in South America during the period of 2008–2009. We generated maps of forest loss, forest gain, consistent forest, and consistent non-forest in South America during 2008–2009.

2.5. Accuracy assessment of PALSAR/MODIS 50-m forest map in 2010

To assess the accuracy of the PALSAR/MODIS forest maps and the other forest maps, we used two sets of validation samples from different

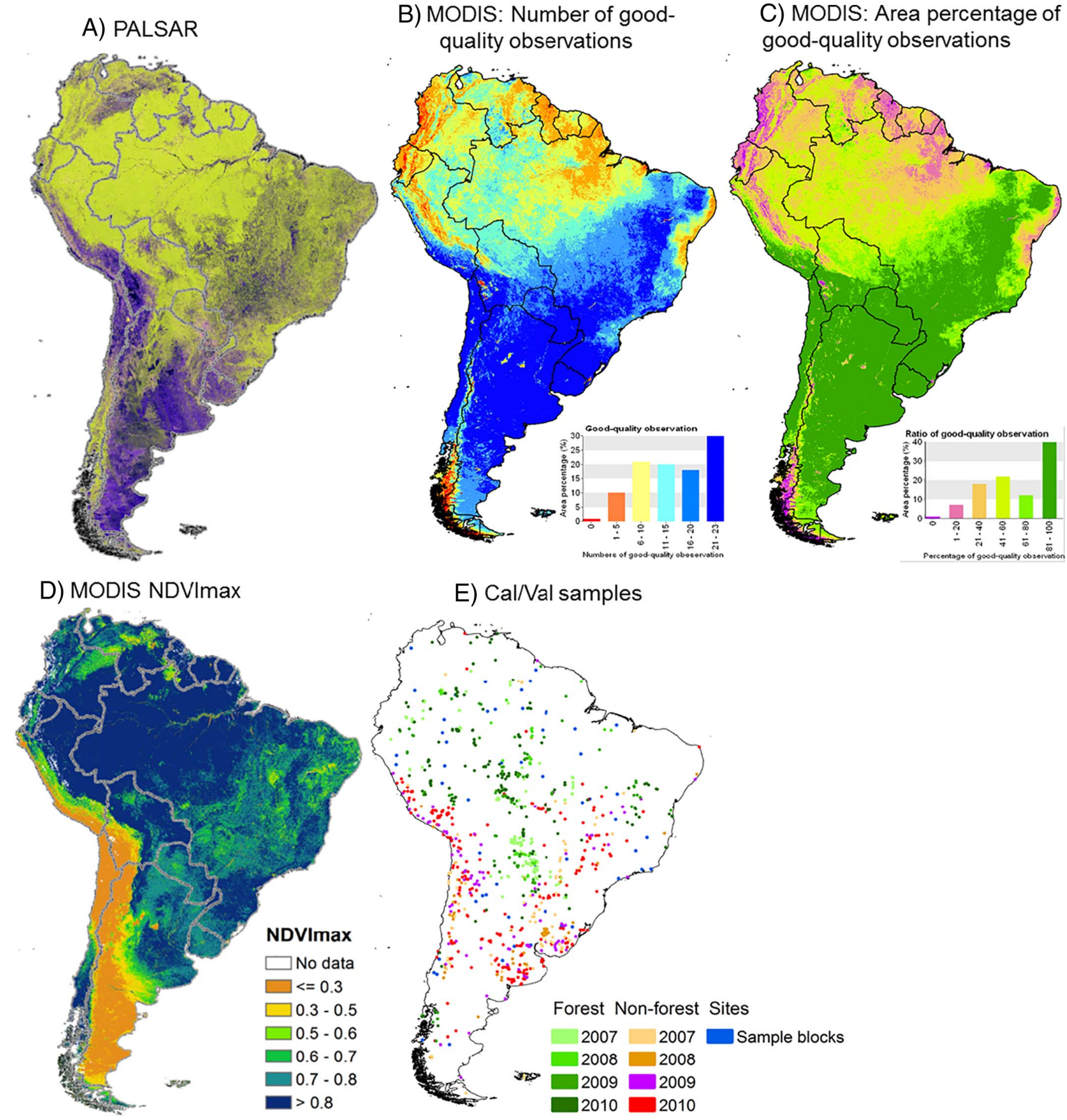

Fig. 2. Input datasets for PALSAR/MODIS forest product. A) The spatial distribution of the false-color composite of ALOS PALSAR in 2010: R (HH), G (HV), and B (HH - HV). B) MODIS: number of good quality observations in 2010; C) MODIS: ratio of good-quality observations in 2010. D) The spatial distribution of MODIS maximum NDVI derived from MOD13Q1 product in year 2010. E) The spatial distribution of the validation samples derived from high resolution images in Google Earth and 55 sample blocks from the Global Land Cover Validation Reference Dataset.

sources, including (1) 500-m by 500-m Region of Interests (ROIs) interpreted from Google Earth images, and (2) the Global Land Cover Validation Reference Dataset from U.S. Geological Survey (USGS) (Olofsson et al., 2012; Pengra et al., 2015; Stehman et al., 2012).

We used the workflow to collect the ground reference data in South America for map accuracy assessment, which was reported in detail in the previous study (Qin et al., 2016). First, we generated twenty 500×500 m ROIs within one 1° by 1° (latitude and longitude) grid cell using a simple random sample approach. Second, we converted those ROIs from the shapefile format into the kml file format and overlaid them on 2.5-m SPOT5 and 2-m WorldView-2 images in Google Earth. The screenshot of the very high spatial resolution (VHR) images within each ROI was automatically downloaded from Google Earth by a freely available software (Quick Macro). Third, we created a protocol for visual interpretation of forest and non-forest ROIs and then provided a training session for researchers participating in data collection. Six

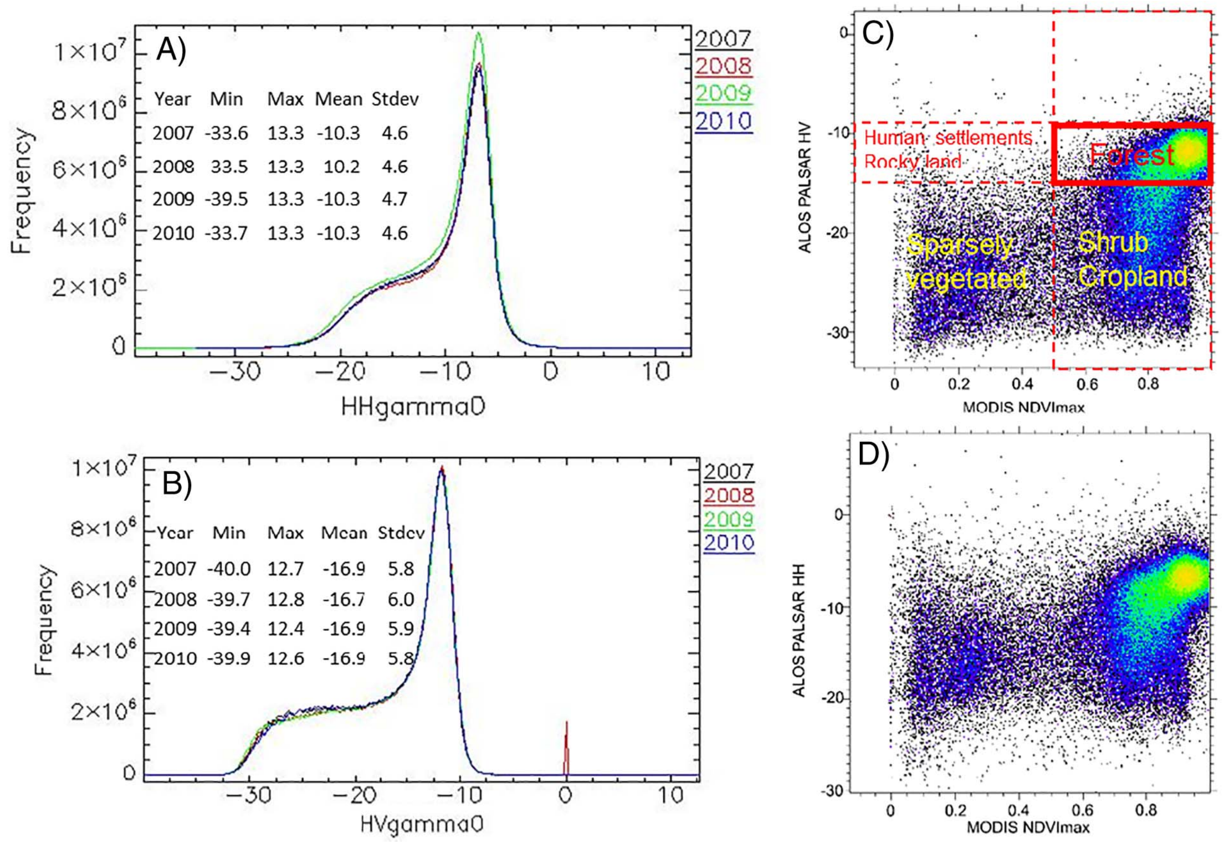

Fig. 3. The distribution of PALSAR HH and HV and MODIS NDVImax in South America. A) and B) The histogram of ALOS PALSAR HH and HV from 2007 to 2010. C) and D) 2-dimension scatter plots of MODIS NDVImax vs ALOS PALSAR HH gamma0 and MODIS NDVImax vs ALOS PALSAR HV gamma0 in South America in 2010.

researchers went through each ROI to identify and delineate forest and non-forest ROI, using these three step procedure. Step 1 is to choose the ROI that is covered by VHR images: If VHR images are not available for a ROI, the interpreters exclude the ROI from visual interpretation. Step 2 is to delineate forest/non-forest ROI. As these 500 × 500 m ROIs were further divided into about 10 × 10 50 × 50 m sub-grids, forest/non-forest ROIs are required to meet one of these two criteria: If a 500 × 500 m ROI is covered by 90% or more tree cover, this ROI is identified as forest; the same criteria applies for non-forest selection. Step 3 is to have quality control of ROIs and visual interpretation. These researchers also served as quality control person for the other researchers and double checked the accuracy of their forest and non-forest selections. After the first-round visual interpretation, we loaded those ROIs and double checked their quality by another group member. Finally, we got 2405 forest ROIs (220,924 pixels) and 2513 non-forest ROIs (256,205 pixels) (Fig. 2E), and 19.7%, 59.5%, and 20.8% of VHR images were acquired during 2007–2010, 2011–2014, and other years, respectively. To reduce the uncertainty from the difference in dates of VHR images, we used the part of selected ROIs in specific year to validate the annual PALSAR/MODIS forest maps, respectively (Section 3.1). We calculated the user's, producer's, and overall accuracy of the PALSAR/MODIS forest maps and their standard errors (Olofsson et al., 2014).

We also analyzed the accuracy for all the forest maps in South America in 2010 using the Global Land Cover Validation Reference Dataset (https://landcover.usgs.gov/glc/SitesDescriptionAndDownloads.php). This dataset was produced from VHR images (QuickBird-2, WorldView-1/2, IKONOS-2, and GeoEye-1) mainly from 2010, collected based on a stratified random sample. There are 55 sites in South America and each of them covers an area of about 5 × 5 km at 2 m resolution. We used four steps to carry out the accuracy assessment as the followings: (1) we grouped the seven land cover classes (tree, water, barren, other vegetation, cloud, shadow, and ice & snow) into three different layers (tree, non-tree, and bad observations) for each site map and then converted their Universal Transverse Mercator (UTM) projection into "equal-area projection" (i.e., South_America_Albers_Equal_Area_Conic); (2) we aggregated the tree, non-tree, and bad observations layers into the same spatial resolutions for each forest map product and calculated their percentage area fraction for each pixel; (3) we excluded those pixels with > 1% area of bad observations; and (4) we used the specific tree cover criteria from 10%, 15%, to 60% to assess the accuracy of different forest maps and calculated their user's, producer's, and overall accuracy and their standard errors (Olofsson et al., 2014).

2.6. Comparison of multiple forest map products in South America

We selected seven forest products for the year 2010, which were freely available to the public and widely used (Fig. 4): 1) The JAXA forest/non-forest map (JAXA): PALSAR FBD data in the growing season in 2010 was used to map forest through region-specific HV threshold values (Shimada et al., 2014). Available at http://www.eorc.jaxa.jp/ALOS/en/palsar_fnf/fnf_index.htm. 2) Landsat tree canopy cover from Global Forest Watch datasets (GFW): time series Landsat ETM + images in main growing season of circa 2010 were used to retrieve 30-m GFW tree cover 2010 through a decision tree algorithm based on the training datasets, selected percentile values, and the slope of linear regression of band reflectance value versus image date (Hansen et al., 2013). Available at https://landcover.usgs.gov/glc/TreeCoverDescriptionAndDownloads.php. 3) Landsat Percent Tree Cover map from Vegetation Continuous Fields (Landsat VCF): the good-quality Global Land Survey (GLS) Landsat images and MODIS cropland layer were included to rescale MODIS VCF into 30-m Landsat VCF using a regression tree model and to improve accuracy in agricultural area (Sexton et al., 2013). Available at http://glcf.umd.edu/data/landsatTreecover/. 4) MODIS VCF: this product was

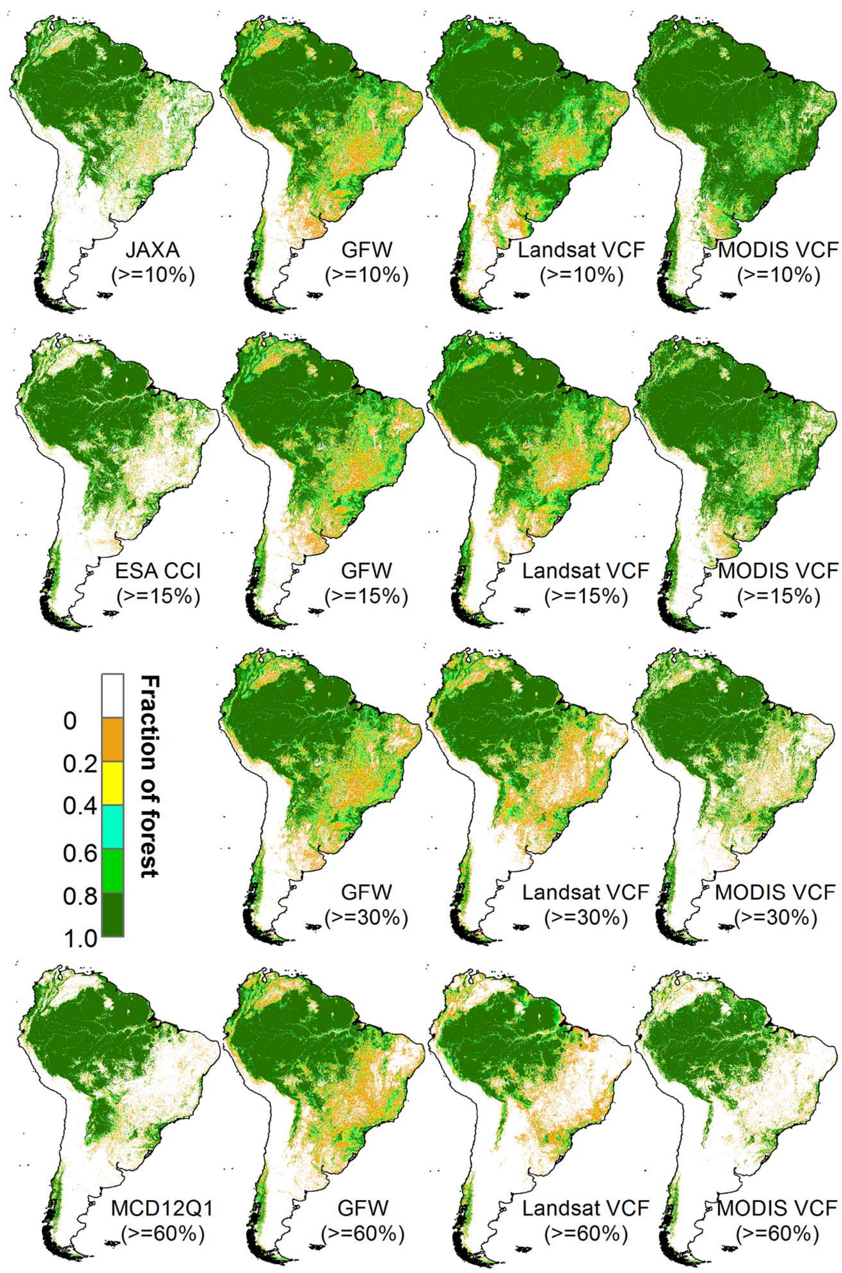

Fig. 4. The spatial distribution of forest fraction cover maps at 1500 m in South America.

generated from the average values of thirty independent VCF products, which were first generated using regression tree models based on the thirty independent samples from the updated training dataset and a 16-day MODIS surface reflectance composite, brightness temperature, and the MODIS Global 250-m Land/Water Map (Townshend et al., 2011). Available at http://glcf.umd.edu/data/vcf/. 5) Land Cover from European Space Agency (ESA) Climate Change Institute (CCI): 300-m time series MEdium Resolution Imaging Spectrometer (MERIS) imagery during 2003–2012 and 1-km SPOT-VEGETATION (2008–2012) time series imagery were used to generate ESA CCI land cover map (European Space Agency, 2016). Available at https://www.esa-landcover-cci.org/?q=node/158. 6) Land Cover Type Yearly L3 Global 500 m SIN Grid (MCD12Q1): 500-m 32-day average nadir bidirectional reflectance distribution function (BRDF)-adjusted land surface reflectance (NBAR), enhanced vegetation index (EVI), land surface temperature (LST), and annual metrics (minimum, maximum, and mean values) for EVI, LST and NBAR bands were used to identify and generate land cover types through a supervised classification approach (Friedl et al., 2010). Available at https://lpdaac.usgs.gov/dataset_discovery/modis/modis_products_table/mcd12q1. 7) Forest Resources Assessment (FRA) from the Food and Agriculture Organization (FAO) of the United Nations: country statistics data of forests in 2010 were collected to generate FAO FRA 2010 (Food and Agriculture Organization of the United Nations, 2012). We compared their total areas and spatial distributions of forests with the PALSAR/MODIS forest map produced in this study in South America. Table 1 summarizes of these forest datasets along with our PALSAR/MODIS forest map.

2.6.1. Area comparison of multiple forest products

We calculated and compared the total forest area from the PASLAR/MODIS forest map and the selected forest products under different percentages of tree cover (≥ 10%, 15%, 30%, 45%, and 60%) as specified by each product's definition of forest at the continental and country scales in South America for 2010. The Root Mean Square Error (RMSE) and linear relationships were calculated to show their differences in forest areas at the country scale:

Table 1
Characteristics of selected forest cover products in South America.

Sensor	Product	Forest definition	Major data source	Spatial resolution	Methods	User's and Producer's accuracy (%)
Statistics	FAO FRA (Food and Agriculture Organization of the United Nations, 2012)	Tree cover ≥ 10%, tree height ≥ 5-m	Country statistics in 2010	Country	Data statistics	
Optical	GFW (Hansen et al., 2013)	Tree cover, tree height ≥ 5-m	30-m Landsat ETM + in circa 2010	30 m	Decision tree	88.4 (± 0.07) and 91.3 (± 0.07)
	Landsat VCF (GLCF) (Sexton et al., 2013)	Tree cover, tree height ≥ 5-m	MODIS VCF, Global Land Survey (GLS) Landsat TM/ETM + from 2008 to 2011	30 m	Regression tree	73.4 (± 0.09) and 94.7 (± 0.11)
	MODIS VCF (DiMiceli et al., 2011)	Tree cover	16-day surface reflectance composite (bands 1–7) and brightness temperature (bands 20, 31, 32) and the MODIS Global 250-m Land/Water Map in 2010.	250 m	Regression tree	72.3 (± 1.05) and 88.1(± 1.13)
	ESA CCI (European Space Agency, 2016)	Tree cover ≥ 15%	300-m land cover map produced by 7-day time series MERIS imagery during 2003–2012 as baseline, 1-km SPOT-VEGETATION (2008–2012) time series for updating	300 m	Unsupervised classification	92.9 (± 0.71) and 72.2 (± 0.42)
	MCD12Q1 (Friedl et al., 2010)	Tree cover ≥ 60%, tree height ≥ 2-m	500-m aggregated 32- day average nadir BRDF-adjusted reflectance (NBAR), enhanced vegetation index (EVI), Land Surface Temperature (LST), and annual metrics (min, max, and mean values) for EVI, LST and NBAR bands in 2010	500 m	Supervised classification	85.7 (± 1.52) and 92.3 (± 1.52)
SAR	JAXA (Shimada et al., 2014)	Tree cover ≥ 10%, tree height ≥ 5-m	50-m ALOS PALSAR in 2010	50 m	Decision tree	95.8 (± 0.08) and 75.1 (± 0.05)
SAR/Optical	PALSAR/MODIS (This study)	Tree cover ≥ 10%, tree height ≥ 5-m	50-m ALOS PALSAR and 250-m MOD13Q1 NDVI in 2010	50 m	Decision tree	95.2 (± 0.09) and 81 (± 0.06)

$$RMSE = \sqrt{\frac{\sum_{t=1}^{n}(x_i - y_i)^2}{n}} \quad (4)$$

where, x_i is the forest area of the ith country from the PASLAR/MODIS forest map in 2010; y_i is the forest area of the ith country from the selected forest product in 2010; n is the total number of countries in South America.

2.6.2. Spatial comparison (pixel level) of multiple forest maps

We applied a cross comparison approach to quantify the spatial consistency and difference between the eight forest maps under different forest definitions. Cross comparison is a method to reveal the uncertainty in global maps where reference data is sparse or not available (Herold et al., 2008). To facilitate the spatial comparison, we first re-projected all the forest maps into equal-area projection (i.e., South_America_Albers_Equal_Area_Conic from ESRI) and then aggregated the 30-m GFW and Landsat VCF forest maps, the 50-m PALSAR/MODIS and JAXA forest maps, the 250-m MODIS VCF forest maps, the 300-m ESA CCI forest map, and the 500-m MCD12Q1 forest map into 1500-m resolution. Each 1500-m pixel has the percentage of forest cover which was averaged from the original datasets. We calculated the forest fraction differences between PALSAR/MODIS forest map and JAXA, GFW, Landsat VCF, and MODIS VCF forest maps defined with tree cover ≥ 10% in South America.

3. Results

3.1. The PALSAR/MODIS tropical forest map of South America in 2010

The PALSAR/MODIS forest map showed the spatial distribution of forests in South America in 2010 (Fig. 5). The Amazon Basin had large areas of forests and most of the land was covered by > 80% forests at the spatial resolution of 1500 m. Northern Colombia, Venezuela, and southeast Brazil were dominated by pasture and savanna ecosystems, but these regions had a small fraction of relatively highly fragmented forests. South America's west coast (Andes Mountains) and southern Argentina had few forests. The overall accuracy of the PALSAR/MODIS forest map for 2010, based on the ground references in 2010 (Table 2), was about 98.01%(± 0.12), and the user's accuracy and the producer's accuracy were about 99.76%(± 0.07) and 95.55%(± 0.07), respectively. The overall, user's, and producer's accuracy of the PALSAR/MODIS forest map in 2010, based on the Global Land Cover Validation Reference Dataset (Table S1), were about 87.13%(± 0.09), 95.15%(± 0.09), and 80.98%(± 0.06), respectively. The total area of the PALSAR/MODIS forests were about 8.63×10^6 km^2 in South America in 2010, or about 48.7% of the total land area. Brazil had the largest forest area about 4.77×10^6 km^2, or about 55% of the total forest area in South America, followed by Peru and Colombia (both with 0.75×10^6 km^2, 8.69%) (Table 3).

3.2. A comparison of the forest cover maps from multiple sources

We compared forest cover at the continental and country scales in South America in 2010 under the definition of tree cover ≥ 10%. At the continental scale, the forest area estimated from the PALSAR/MODIS forest map (8.63×10^6 km^2) was similar to FAO FRA (8.64×10^6 km^2) and JAXA (8.19×10^6 km^2) forest products, but much smaller than GFW (9.56×10^6 km^2), Landsat VCF (11.50×10^6 km^2), and MODIS VCF (12.70×10^6 km^2) (Fig. 6A). At the country scale, the PALSAR/MODIS forest map had very good linear relationships with JAXA, Giri (Giri and Long, 2014), FAO FRA, and GFW in forest area estimates, with the slope ranging from 0.92 to 1.09 and a RMSE range from 0.05×10^6 km^2 to 0.13×10^6 km^2 (Fig. 6B). Landsat VCF and MODIS VCF overestimated about 29% and 46% of total forest area, respectively, and had relatively larger RMSEs (0.40×10^6 km^2 and 0.63×10^6 km^2), especially in Brazil (1.37×10^6 km^2 and

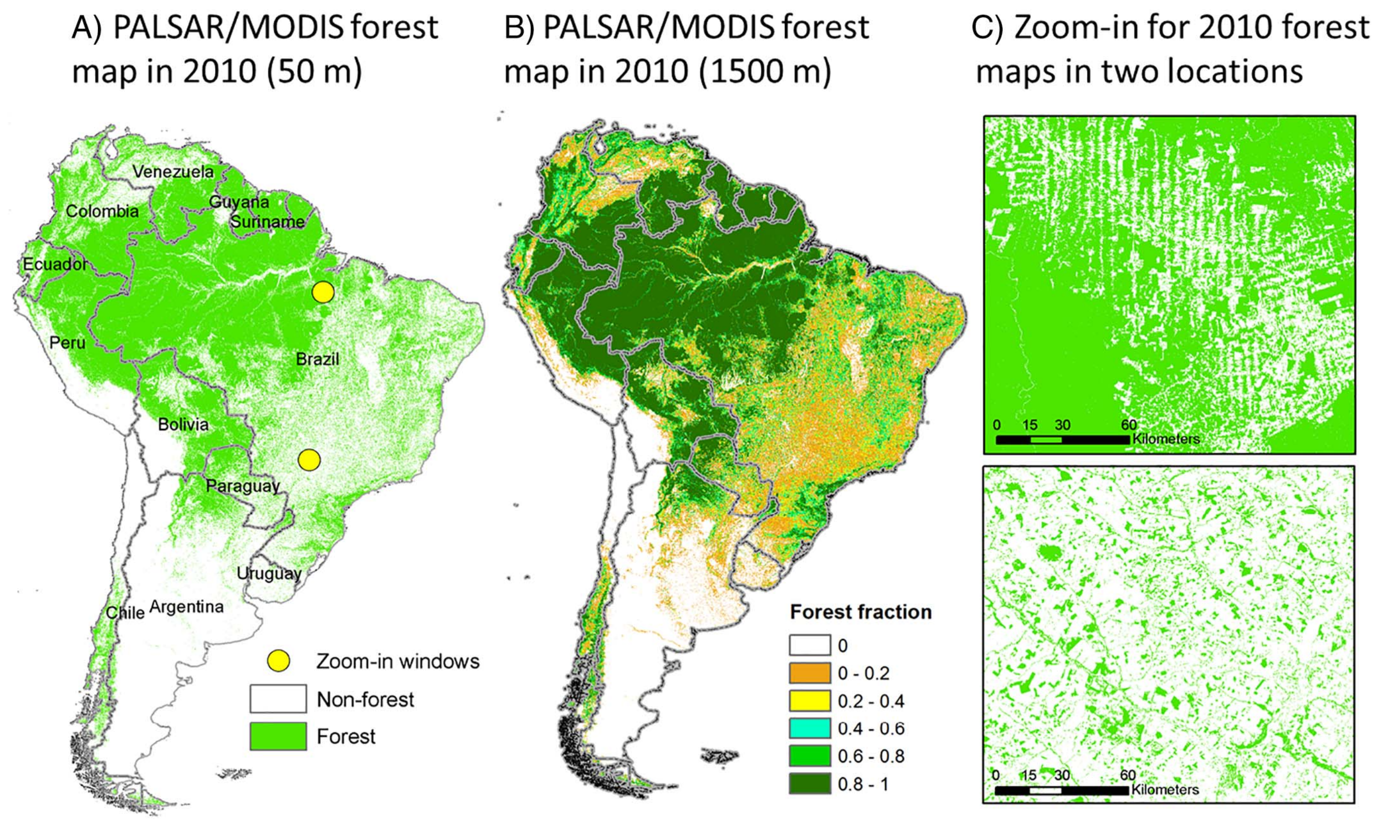

Fig. 5. The spatial distribution of the PALSAR/MODIS forest map in South America in 2010.

2.24×10^6 km^2) and Argentina (0.39×10^6 km^2 and 0.62×10^6 km^2) (Fig. 6C).

We evaluated the consistency among the eight maps at the pixel scale (Fig. 7). PALSAR/MODIS forest map and JAXA forest map showed very good agreement in their spatial distribution and about 90% of the pixels were in agreement on forest cover (Fig. 7A). The PALSAR/MODIS forest map had lower forest cover in the northern region of South America than the JAXA forest map, where the landscape is dominated by sparsely vegetated land, and had higher forest cover in the sub-humid and subtropical regions than the JAXA forest map. The PALSAR/MODIS forest map in 2010 had relatively large differences in the spatial distribution of forests when compared to optical remote sensing based forest maps (GFW, Landsat VCF, and MODIS VCF) for South America. The GFW and PALSAR/MODIS forest maps were in close agreement in the spatial distribution of forest cover with about 86% of the pixels being consistent (Fig. 7B). When compared with PALSAR/MODIS forest cover, Landsat VCF and MODIS VCF overestimated forest cover extensively at the edge of rainforest and in the semi-humid and subtropical regions, with only about 69% and 60% of forest pixels being consistent (Fig. 7C and D).

3.3. Annual loss, gain, and net change of forest areas in South America during 2008–2009

The total area and spatial distribution of the PALSAR/MODIS forest maps were relatively stable and consistent in South America between 2008 and 2009 (Figs. 8–9). Consistent forest and non-forest areas were 8.50×10^6 km^2 and 8.87×10^6 km^2, respectively, which is about 47.95% and 50.04% of the total land area in South America. Analyses of PALSAR/MODIS forest maps in 2008 and 2009 showed a small net loss in total forest cover of about 0.39% of the total forest area in South America (0.32×10^5 km^2 year^{-1}). The annual rates of forest loss

Table 2
Accuracy assessment for the PALSAR/MODIS forest maps.

Year	Classification	Ground reference			User's accuracy (%)	Producer's accuracy (%)	Overall accuracy (%)
		Forest	Non-forest	Total			
2007	Forest	9591	107	9698	98.90 (± 0.21)	94.77 (± 0.19)	96.72 (± 0.25)
	Non-forest	529	9190	9719	94.56 (± 0.45)	98.85 (± 0.47)	
	Total	10,120	9297	19,417			
2008	Forest	4713	10	4723	99.79 (± 0.13)	98.29 (± 0.13)	99.21 (± 0.15)
	Non-forest	82	6799	6881	98.81 (± 0.26)	99.85 (± 0.26)	
	Total	4795	6809	11,604			
2009	Forest	8395	36	8431	99.57 (± 0.14)	92.67 (± 0.12)	96.48 (± 0.23)
	Non-forest	664	10,812	11,476	94.21 (± 0.43)	99.67 (± 0.45)	
	Total	9059	10,848	19,907			
2010	Forest	16,925	41	16,966	99.76 (± 0.07)	95.55 (± 0.07)	98.01 (± 0.12)
	Non-forest	788	23,996	24,784	96.82 (± 0.22)	99.83 (± 0.22)	
	Total	17,713	24,037	41,750			

Table 3
The forest area in different countries and regions in South America from multiple data sources in 2010 ($\times 10^6$ km^2).

Tree cover		BRA	COL	PER	BOL	VEN	ARG	GUY	PRY	ECU	CHL	SUR	French Guiana	URY	Falkland Islands	Total area
≥ 10%	PALSAR/MODIS	4.77	0.75	0.75	0.60	0.55	0.28	0.19	0.18	0.17	0.16	0.13	0.08	0.01	0.00	8.63
	JAXA	4.36	0.78	0.76	0.59	0.57	0.22	0.19	0.15	0.17	0.17	0.14	0.08	0.01	0.00	8.19
	GFW	5.20	0.84	0.80	0.65	0.59	0.42	0.19	0.22	0.20	0.21	0.14	0.08	0.02	0.00	9.56
	Landsat VCF	6.14	1.04	0.83	0.74	0.75	0.68	0.20	0.32	0.21	0.30	0.14	0.08	0.07	0.01	11.50
	MODIS VCF	7.01	0.99	0.85	0.75	0.77	0.91	0.20	0.35	0.22	0.31	0.14	0.08	0.10	0.01	12.70
	Giri	4.91	0.76	0.78	0.64	0.54	0.37	0.19	0.22	0.18	0.21	0.14	0.08	0.02	–	9.03
	FAO FRA	5.2	0.60	0.68	0.57	0.46	0.29	0.15	0.18	0.10	0.16	0.15	0.08	0.02	0.00	8.64
≥ 15%	ESA CCI	4.17	0.65	0.78	0.60	0.44	0.34	0.18	0.22	0.16	0.18	0.14	0.08	0.01	0.00	7.94
	GFW	5.19	0.84	0.79	0.65	0.59	0.42	0.19	0.22	0.20	0.20	0.14	0.08	0.02	0.00	9.53
	Landsat VCF	5.19	0.95	0.79	0.66	0.69	0.44	0.19	0.25	0.19	0.25	0.14	0.08	0.02	0.00	9.85
	MODIS VCF	5.93	0.89	0.81	0.68	0.70	0.59	0.19	0.29	0.20	0.28	0.14	0.08	0.04	0.01	10.83
≥ 30%	GFW	4.97	0.81	0.79	0.63	0.57	0.38	0.19	0.20	0.19	0.20	0.14	0.08	0.02	0.00	9.17
	Landsat VCF	4.07	0.72	0.73	0.54	0.53	0.19	0.18	0.09	0.14	0.18	0.14	0.08	0.01	0.00	7.60
	MODIS VCF	4.31	0.69	0.75	0.54	0.55	0.24	0.17	0.11	0.15	0.20	0.14	0.08	0.01	0.00	7.94
≥ 45%	GFW	4.68	0.78	0.77	0.59	0.54	0.31	0.19	0.17	0.18	0.18	0.14	0.08	0.02	0.00	8.64
	Landsat VCF	3.67	0.60	0.71	0.46	0.45	0.10	0.17	0.04	0.12	0.15	0.13	0.08	0.01	0.00	6.69
	MODIS VCF	3.79	0.58	0.72	0.46	0.46	0.12	0.15	0.04	0.13	0.16	0.13	0.08	0.01	0.00	6.82
≥ 60%	GFW	4.26	0.74	0.76	0.52	0.49	0.17	0.19	0.09	0.16	0.17	0.14	0.08	0.01	0.00	7.78
	Landsat VCF	3.31	0.50	0.66	0.40	0.38	0.06	0.14	0.02	0.10	0.13	0.13	0.07	0.00	0.00	5.91
	MODIS VCF	3.29	0.50	0.67	0.38	0.38	0.07	0.12	0.01	0.10	0.13	0.12	0.07	0.00	0.00	5.83
	MOD12Q1	3.65	0.67	0.75	0.51	0.44	0.31	0.19	0.15	0.15	0.21	0.14	0.08	0.01	0.00	7.25

Short names for countries: BRA (Brazil), COL (Colombia), PER (Peru), BOL (Bolivia), VEN (Venezuela), ARG (Argentina), GUY (Guyana), PRY (Paraguay), ECU (Ecuador), CHL (Chile), SUR (Suriname), and URY (Uruguay).

(1.95×10^5 km^2 year^{-1}) and gain (1.62×10^5 km^2 year^{-1}) were high, about 2.34% and 1.95% of the total forest area, respectively. Therefore, our results suggest that forests went through extensive disturbance in South America. Brazil had the largest rates of forest loss (1.07×10^5 km^2 year^{-1}) and gain (0.95×10^5 km^2 year^{-1}) out of all South American countries. Brazil and Argentina had the largest rate of net forest loss at about 0.11×10^5 km^2 year^{-1} and 0.08×10^5 km^2 year^{-1}, respectively. The forest loss moved from the forest edges into the Amazon Basin area where intact forests were dominated.

4. Discussion

4.1. The need for accurate forest cover maps by user communities

Forest types, areas, and biophysical parameters (e.g., canopy height, biomass, and leaf area index) is important information for user communities whose efforts have been to reduce carbon dioxide emissions, enhance terrestrial carbon sequestration, and protect biodiversity from deforestation and forest degradation (REDD +). The user communities have used different forest cover maps to investigate the degradation in the carbon stocks near tropical forest edges (Chaplin-Kramer et al., 2015) and habitat fragmentation (Haddad et al., 2015). In this study, we compared the total area and spatial distribution of multiple forest cover products. The results showed that large uncertainties existed among these forest products, especially in those areas with relatively low forest cover. These uncertainties could affect the perception of user communities on studies that investigated the effects of forest areas and fragmentation on carbon cycle, biodiversity, and conservation. For example, a recent study in Rondonia, Brazil assessed how the extent and configuration of remnant forests in replicate 10,000 ha landscapes had affected the occurrence of some Amazonian mammals and birds (Ochoa-Quintero et al., 2015). Those regions with low forest cover (i.e., seasonally dry forest) often harbor high biodiversity but their forests are highly threatened with only 10% of their original extent remaining in many countries (Banda-R et al., 2016). Therefore, it is imperative to have accurate and updated forest cover maps at high spatial resolutions (< 100 m) with reduced uncertainty. Several studies have investigated what factors contribute the most to the uncertainties of forest cover maps at regional and global scales (Kaptue Tchuente et al., 2011; Sexton et al., 2013). Forest definition was considered to be the major contribution to the uncertainty and difference in the area and spatial distribution of forests among various global forest cover maps (Sexton et al., 2015). Other studies suggested that image data and mapping algorithms are also important factors (Dong et al., 2012; Kaptue Tchuente et al., 2011; Qin et al., 2016; Qin et al., 2015).

4.2. Improved forest cover maps from (1) optical images and (2) vegetation continuous field (VCF) concept

It is challenging to accurately map forests from optical images with coarse spatial resolutions in heterogeneous landscapes (Lu and Weng, 2007). The 500-m or 250-m MODIS and 300-m MERIS datasets could overestimate or under-estimate forest area and spatial extent in landscapes with low tree cover and these datasets are not sensitive to fragmentation caused by selective logging (Fig. 10) (Asner et al., 2005). Compared to high spatial resolution forest maps, coarse spatial resolution forest maps overestimate dense forest area and forest edge but underestimate areas that are sparsely forested (Figs. 4 and 10). Based on the analysis of 55 Global Land Cover Validation Reference Dataset site maps, high spatial resolution forest maps can capture the details of land cover and reduce the number of mixed pixels. About 45%, 15%, and 40% of their pixels have tree cover values between 0 and 0.1, 0.1–0.9, and 0.9–1.0, respectively. While coarse spatial resolution forest maps have more mixed pixels, about 35%, 30%, and 35% of pixels have tree cover values between 0 and 0.1, 0.1–0.9, and 0.9–1.0, respectively. Previous studies showed that sparsely forested areas have relatively large uncertainty (Sexton et al., 2015), therefore, coarse spatial resolution forest maps are likely to have more uncertainty in forest area and spatial patterns. From Fig. 6A, high spatial resolution forest maps have relatively small forest area ranges and coarse spatial resolution forest maps have relatively large forest area ranges.

In recent years, the VCF concept has been widely used in land cover mapping and three global VCF-based forest cover data products have been generated: MODIS VCF (DiMiceli et al., 2011), Landsat VCF (Sexton et al., 2013), and GFW (Hansen et al., 2013). As shown in Fig. 6A, when a 45% VCF threshold value is used, the total forest area estimated from the GFW (8.64×10^6 km^2) is very close to the forest area estimates from the FAO FRA 2010 (8.64×10^6 km^2), JAXA PALSAR (8.19×10^6 km^2), and PALSAR/MODIS (8.63×10^6 km^2) products, which all use 10% forest area cover in forest definition. This agreement between GFW (45%) and PALSAR-based forest maps is not a coincidence. Optical and microwave remote sensing images measure

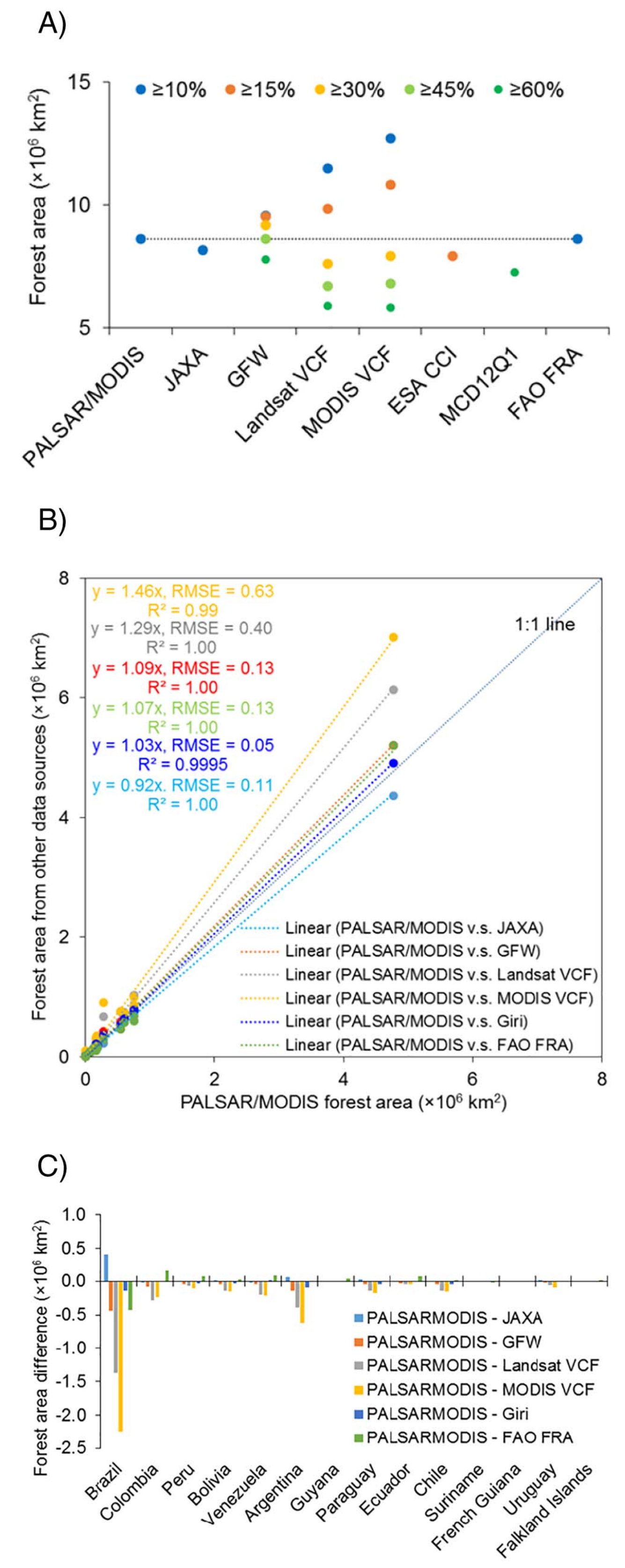

Fig. 6. A comparison of forest cover areas at the continental (A) and country scales (B and C) in 2010.

different components of forests. Optical remote sensing images (e.g., MODIS, Landsat) are mostly related to vegetation canopy (tree crown canopy, leaves, and leaf area index), greenness, and phenology. L-band microwave remote sensing images (e.g., PALSAR) penetrates through the forest canopy (leaves) and interacts with tree branches and trunks. Forests usually have leaf area index values of 4 m^2/m^2 and higher, thus vegetation canopy (tree crown canopy) have much larger areas than tree trunks and branches (projected areas). Forest products have close forest estimation in the areas with relatively high leaf area index ($\geq 4\ m^2/m^2$). MODIS VCF and Landsat VCF have more forests with relatively low leaf area index ($< 4\ m^2/m^2$) than those of GFW, PALSAR/MODIS, and JAXA in the areas (Fig. 11). This difference suggests that when the VCF datasets are used to estimate total forest area and compared with the FAO FRA total forest area estimates (10% tree cover in its forest definition), one needs to consider leaf area index as an adjusting factor and use much higher (e.g., 30% to 60% for GFW, 15%–30% for both MODIS VCF and Landsat VCF) threshold values in the VCF datasets to estimate forest cover.

4.3. Improved forest cover maps from (1) the integration of microwave (PALSAR) and optical images, and (2) the phenology concept

Microwave remote sensing is not affected by frequent clouds and has substantial advantages for mapping tropical forests, especially in the humid tropical area. The L-band JERS-1 HH polarization dataset in late 1995 was used to generate forest cover maps in the Amazon Basin based on a supervised classification approach and a hierarchical decision rule (Saatchi et al., 2000). In recent years, L-band ALOS PALSAR HH and HV polarization datasets in 2007–2010 were used to produce global forest maps based on specific region decision rules (Shimada et al., 2014). As human settlements (e.g., buildings) and rocky lands usually have similar HH or HV values as forests, there is a need to identify them and reduce the commission error of forest cover maps (Dong et al., 2012; Qin et al., 2015). We have evaluated the methods that use PALSAR and optical images (e.g., Landsat, MODIS) to identify buildings and rocky lands (Qin et al., 2017; Qin et al., 2016). We have combined PALSAR and MODIS images to map forest cover in 2010 in China (Qin et al., 2015) and monsoon Asia (Qin et al., 2016). The forest area estimated for China in 2010 ($2.02 \times 10^6\ km^2$) from the PALSAR/MODIS approach is very close to the forest area estimate from the China National Forestry Inventory ($1.95 \times 10^6\ km^2$) and FAO FRA-2010 ($2.07 \times 10^6\ km^2$) (Qin et al., 2015). The forest area estimated for monsoon Asia (23 countries) in 2010 ($6.32 \times 10^6\ km^2$) from the PALSAR/MODIS approach is also close to the forest area estimate from the FAO FRA-2010 ($5.80 \times 10^6\ km^2$) (Qin et al., 2016). In this study, the forest area estimated for South America in 2010 ($8.63 \times 10^6\ km^2$) from the PALSAR/MODIS approach is also very close to the forest area estimate from the FAO FRA-2010 ($8.64 \times 10^6\ km^2$). Many studies have recognized the issue of large uncertainties in forest cover estimates and called for the integration of optical and microwave remote sensing images as a potential way to improve the accuracy of tropical forest maps (Espirito-Santo et al., 2010; Reiche et al., 2015). Our previous efforts for China (Qin et al., 2015), monsoon Asia (Qin et al., 2016), and this study's efforts for South America have clearly demonstrated the potential of integrating PALSAR and MODIS images to generate updated and accurate forest cover maps at the country and continental scales. These results also show that the FAO FRA-2010 dataset, which is based on forest inventory from individual countries, is a reasonably reliable dataset for the studies at country and continental scales.

Our study uses both PALSAR images (sensitive to structure- and biomass of forests) and MODIS NDVI imagery (sensitive to canopy leaf area index and phenology). ALOS satellite (PALSAR) was launched in 2006 and failed to work by April 2011. It provided global (excluding Antarctica > 77.5° South latitude) and high resolution (50-m and 25-m) L-band FBD mosaic datasets from 2007 to 2010 (Rosenqvist et al., 2014). ALOS-2 satellite (PALSAR-2) was launched in May 2014,

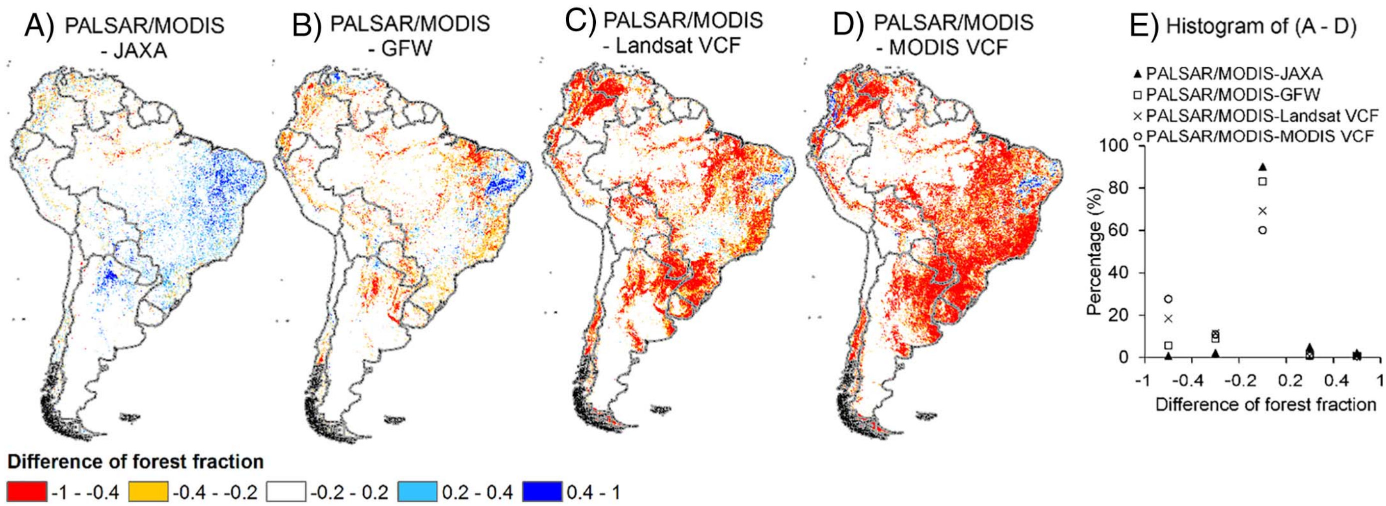

Fig. 7. The spatial distribution of multiple forest cover maps and their difference at the resolution of 1500 m.

equipped with enhanced L-band SAR sensors and plan to provide the global observation up to the year 2021. PALSAR-2 global L-band FBD mosaic datasets in 2015 and 2016 are freely available to the public. The availability of both PALSAR and PALSAR-2 images opens a new opportunity to apply our mapping method to track and quantify spatial patterns and temporal changes of forests in South America and other parts of the world.

4.4. Forest cover dynamics in South America

Quantifying and mapping annual changes in forest cover (loss, gain, and net change) is important for forest resource management but remains highly debated with large uncertainty. For example, according to the FAO FRA reports, the average annual net change of total forest cover in South America was a loss of $40.0 \times 10^3\,km^2\,year^{-1}$ in 1990–2000, $44.4 \times 10^3\,km^2\,year^{-1}$ in 2000–2005, $33.0 \times 10^3\,km^2\,year^{-1}$ in 2005–2010, and $20.2 \times 10^3\,km^2\,year^{-1}$ in 2010–2015, respectively (Keenan et al., 2015). The difference between the PALSAR/MODIS forest maps in 2008 and 2009 also gave a relatively small annual net change in total forest cover (a loss of $32.4 \times 10^3\,km^2\,year^{-1}$) in South America. This demonstrates the complementary values of PALSAR/MODIS forest maps to the FAO FRA effort at continental scale. At the country scale, the net change in forest area from the PALSAR/MODIS forest maps in 2008–2009 differ from the FAO FRA 2010 dataset, with relatively large differences in Brazil ($11.5 \times 10^3\,km^2\,year^{-1}$ versus $16.6 \times 10^3\,km^2\,year^{-1}$), Argentina ($8.4 \times 10^3\,km^2\,year^{-1}$ versus $3.2 \times 10^3\,km^2\,year^{-1}$), and Bolivia ($1.5 \times 10^3\,km^2\,year^{-1}$ versus $5.1 \times 10^3\,km^2\,year^{-1}$) (Fig. 9A). Given the large areas of forest cover and remoteness in Brazil and Argentina, the forest inventory approach for the FAO FRA 2010 data product is likely to have higher uncertainty than do the PALSAR/MODIS forest maps.

Several studies reported that the tropical forests of South America had the largest loss in forest cover, driven by clear-cut logging, selective logging, and the conversion of forests to pasture and croplands (De Sy et al., 2015; Hansen et al., 2013). In Brazil, the GFW reported annual forest losses in 2008 ($80.7 \times 10^3\,km^2$) and 2009 ($81.8 \times 10^3\,km^2$), which was based on analyses of Landsat images (Fig. 9B). These losses are much smaller than the total forest loss calculated from PALSAR/MODIS maps in 2008 and 2009 ($194.6 \times 10^3\,km^2$). The discrepancy

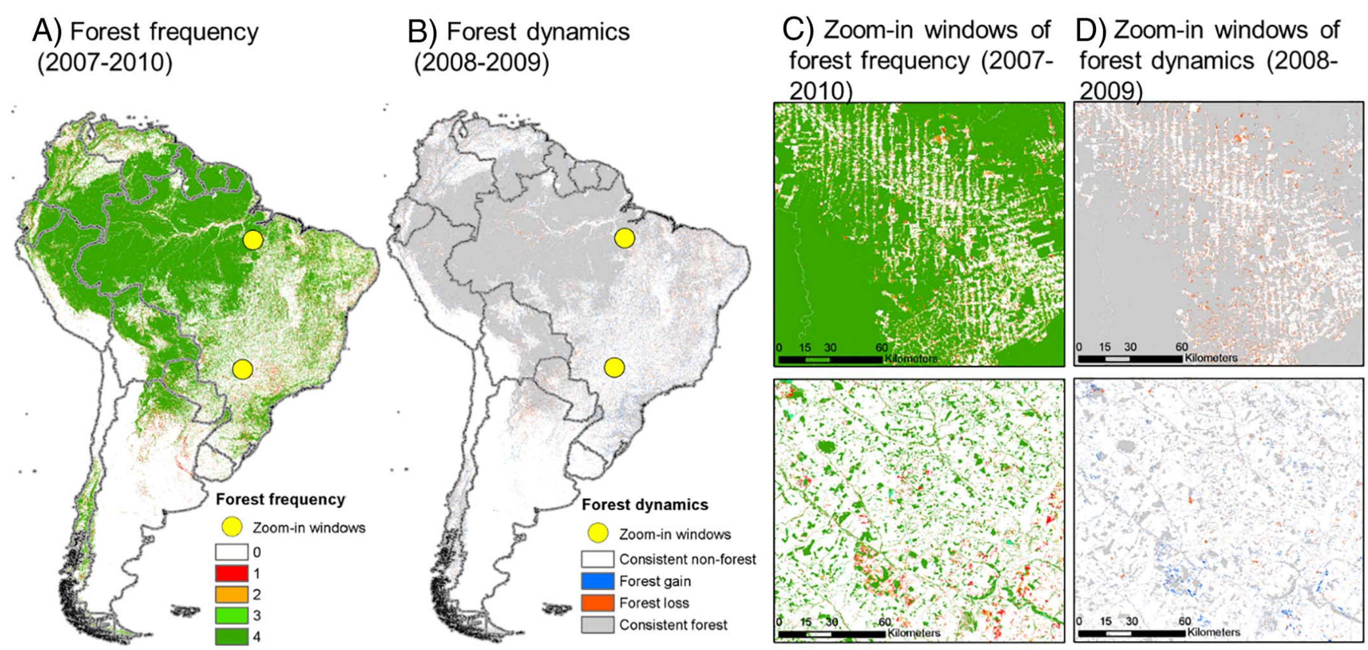

Fig. 8. Forest frequency and dynamics of the PALSAR/MODIS forest maps in South America.

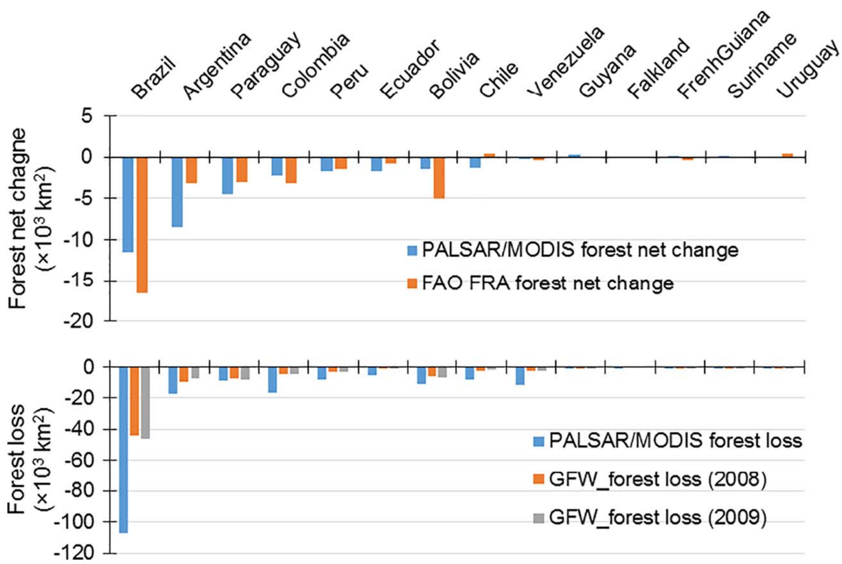

Fig. 9. The area changes of the PALSAR/MODIS forest maps in South America during 2008-2009.

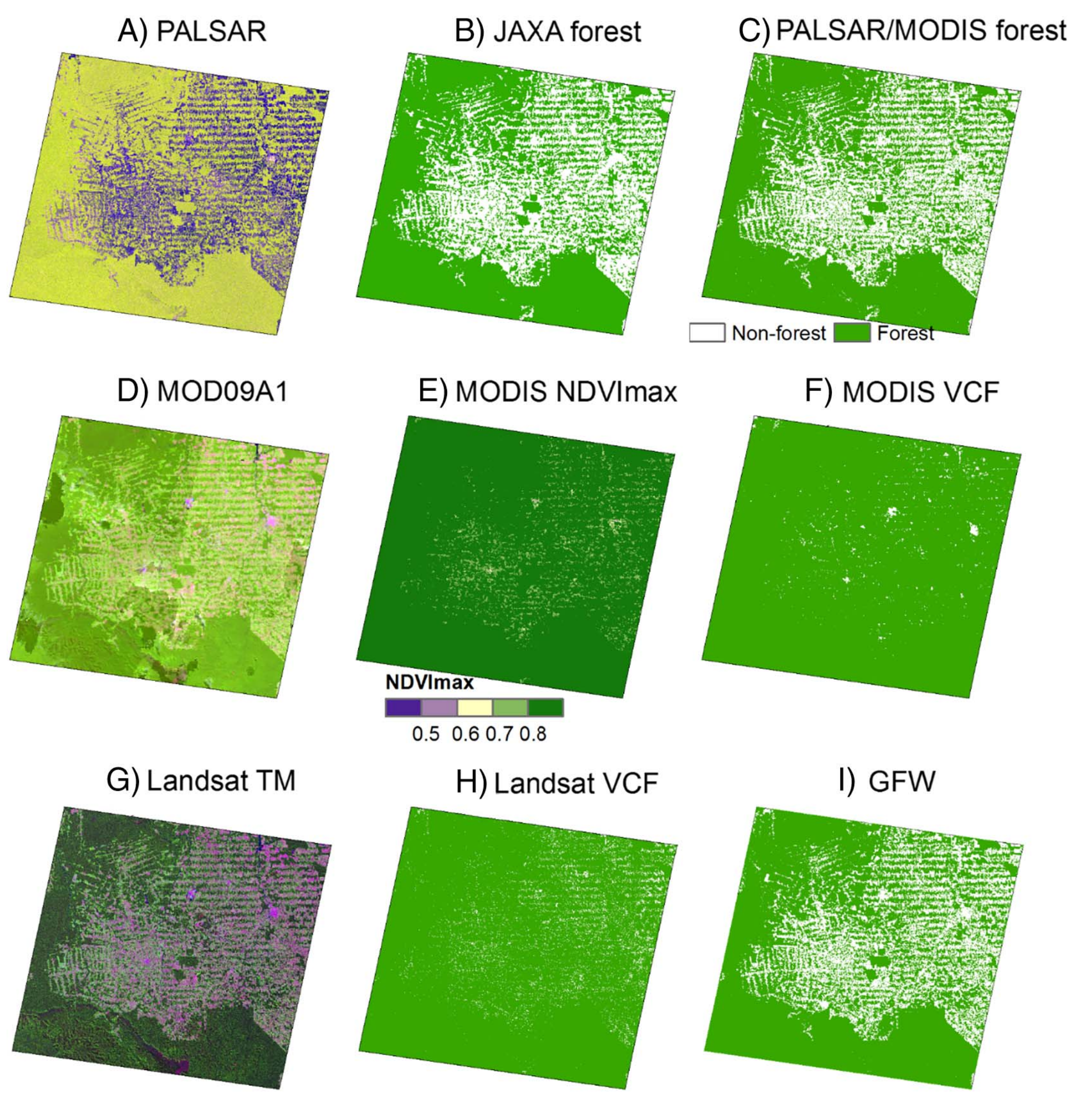

Fig. 10. Forest edges. A) False color composition of PALSAR image, with R (HH), G (HV), and B (HH-HV). B) 50-m JAXA forest/non-forest map. C) 50-m PALSAR/MODIS forest/non-forest map. D) False color composition of MODIS land surface reflectance, acquired on May 9, 2010, with R (SWIR2), G (NIR), and B (Red). E) 250-m MODIS maximum NDVI. F) 250-m forest map from MODIS VCF (tree cover ≥ 10%). G) False color composition of 30-m Landsat TM image, acquired on May 15, 2010, with R (SWIR1), G (NIR), and B (Red). H) 30-m forest map from Landsat VCF (tree cover ≥ 10%). I) 30-m forest map from GFW (tree cover ≥ 10%).

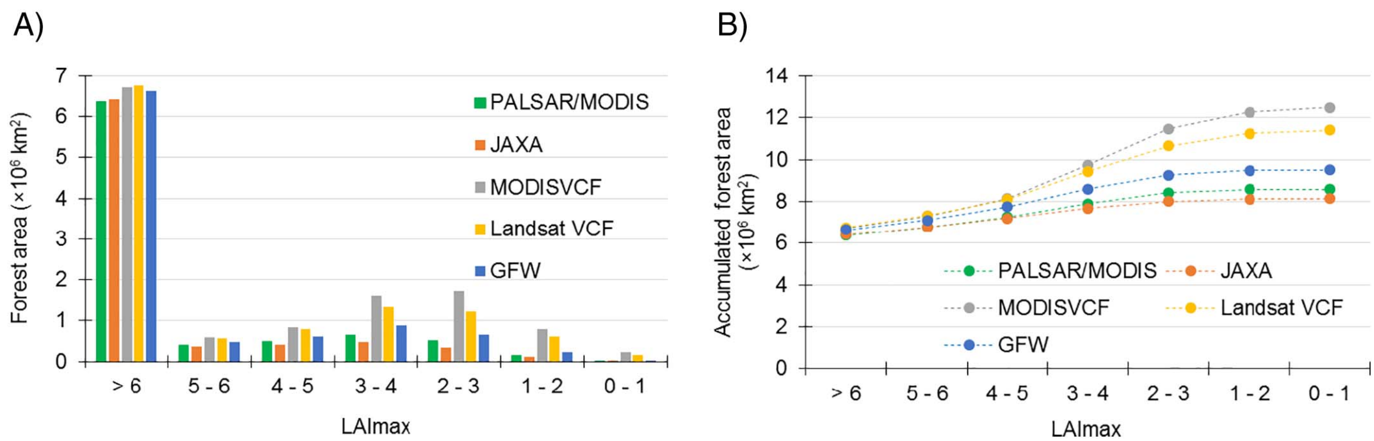

Fig. 11. Forest area (tree cover ≥ 10%) within different ranges of the annual maximum leaf area index (LAImax) in South America in 2010. LAImax is calculated from the MODIS LAI product (MCD15A3H.006 Terra + Aqua Leaf Area Index/FPAR 4-Day L4 Global 500 m).

between GFW and our PALSAR/MODIS maps can be attributed to several reasons, including the mapping algorithms and image data used. Forest fires from natural and anthropogenic sources are an indicator of forest cover loss. The burned area was estimated to be about $200 \times 10^3\,km^2$ and $250 \times 10^3\,km^2$ in 2008 and 2009 in South America, respectively (Randerson et al., 2012). Severe weather, such as wind storms (Espirito-Santo et al., 2010) and drought (Phillips et al., 2009), had also caused large losses or disturbance in forest cover. Furthermore, the short-rotation industrial forest plantations such as Eucalyptus plantations is another factor complicating the calculation and mapping of forest cover (loss and gain) (le Maire et al., 2014). The short-rotation Eucalyptus replaced natural forests and expanded quickly in South America. For example, the Eucalyptus plantation area in Brazil increased from $35 \times 10^3\,km^2$ in 2006 to about $50 \times 10^3\,km^2$ in 2010 (ABRAF, 2012).

According to the accuracy assessment from Global Land Cover Validation Reference Dataset site maps, the PALSAR/MODIS forest maps can capture dense forest very well and are not very sensitive to the sparse forests, which may affect the identification of sparse forest changes. Although it is difficult to use either high spatial resolution images or ground reference data to assess the annual dynamics of forest areas (loss, gain, and net change) from the PALSAR/MODIS forest maps due to the limited data availability, the PALSAR/MODIS forest maps do serve as complimentary datasets to both FAO FRA and GFW products at the continental and country scales.

5. Conclusion

Accurate forest cover maps in South America are critical datasets for biodiversity and conservation management, assessing changes in the carbon and water cycle, and determining the effects of a changing climate. However, several global forest cover maps derived from analyses of optical images have large uncertainties (Sexton et al., 2015). In this study, we integrated optical (MODIS) and microwave (PALSAR) remote sensing images and produced annual forest cover maps at 50-m spatial resolution in 2007–2010 with high accuracy. The comparison by this study of the total areas and spatial extents reported by multiple forest cover map products has shown that: (1) there is little uncertainty in forest cover in the areas of the Amazon Basin with dense forest cover: (2) there is large uncertainty in forest cover in the semi-humid regions with sparse forest cover and at the forest edges; (3) all forest maps tend to underestimate forests in the areas with relatively low tree cover, especially for the forest maps generated by coarse spatial resolution images; optical-based VCF products are easy to overestimate forests in the area with tree cover < 10%, especially for MODIS VCF and Landsat VCF, and microwave/optical-based forest product has much improvement; (4) PALSAR/MODIS forest maps in 2008/2009 report much larger forest dynamics (gain, loss) than GFW did. The large discrepancies in these forest cover products suggest that the researchers and the decision makers should be cautious in choosing forest cover map products. As Landsat and Sentinel-2 images are also available, future studies of forest cover maps should also explore the integration of microwave (PALSAR, PALSAR-2) and optical (MODIS, Landsat, and Sentinel-2) images and track the spatio-temporal changes of forests (Chen et al., 2016; Dong et al., 2013; Reiche et al., 2015).

Acknowledgements

This work was carried out with the support of research grants from the Inter-American Institute for Global Change Research (IAI) (CRN3076), which is supported by the US National Science Foundation (GEO-1128040), the National Aeronautics and Space Administration (NASA) Land Cover and Land Use Change program (NNX14AD78G), the National Science Foundation (NSF) EPSCoR program (IIA-1301789). We thank Sarah Xiao at Yale University for English editing of the manuscript.

Appendix A. Supplementary data

Supplementary data to this article can be found online at http://dx.doi.org/10.1016/j.rse.2017.09.005.

References

ABRAF, 2012. Chapter 01, planted forests in Brazil. In: Statistical Yearbook 2012.
Achard, F., Eva, H., Mayaux, P., 2001. Tropical forest mapping from coarse spatial resolution satellite data: production and accuracy assessment issues. Int. J. Remote Sens. 22, 2741–2762.
Achard, F., DeFries, R., Eva, H., Hansen, M., Mayaux, P., Stibig, H.J., 2007. Pan-tropical monitoring of deforestation. Environ. Res. Lett. 2.
Asner, G.P., 2001. Cloud cover in Landsat observations of the Brazilian Amazon. Int. J. Remote Sens. 22, 3855–3862.
Asner, G.P., Knapp, D.E., Broadbent, E.N., Oliveira, P.J.C., Keller, M., Silva, J.N., 2005. Selective logging in the Brazilian Amazon. Science 310, 480–482.
Baccini, A., Goetz, S.J., Walker, W.S., Laporte, N.T., Sun, M., Sulla-Menashe, D., Hackler, J., Beck, P.S.A., Dubayah, R., Friedl, M.A., Samanta, S., Houghton, R.A., 2012. Estimated carbon dioxide emissions from tropical deforestation improved by carbon-density maps. Nat. Clim. Chang. 2, 182–185.
Ban, Y.F., 2003. Synergy of multitemporal ERS-1 SAR and Landsat TM data for classification of agricultural crops. Can. J. Remote. Sens. 29, 518–526.
Banda-R, K., Delgado-Salinas, A., Dexter, K.G., Linares-Palomino, R., Oliveira-Filho, A., Prado, D., Pullan, M., Quintana, C., Riina, R., Rodríguez, M.G.M., Weintritt, J., Acevedo-Rodríguez, P., Adarve, J., Álvarez, E., Aranguren, B.A., Arteaga, J.C., Aymard, G., Castaño, A., Ceballos-Mago, N., Cogollo, Á., Cuadros, H., Delgado, F., Devia, W., Dueñas, H., Fajardo, L., Fernández, Á., Fernández, M.Á., Franklin, J., Freid, E.H., Galetti, L.A., Gonto, R., González-M., R., Graveson, R., Helmer, E.H., Idárraga, Á., López, R., Marcano-Vega, H., Martínez, O.G., Maturo, H.M., McDonald, M., McLaren, K., Melo, O., Mijares, F., Mogni, V., Molina, D., Moreno, N.d.P., Nassar, J.M., Neves, D.M., Oakley, L.J., Oatham, M., Olvera-Luna, A.R., Pezzini, F.F., Dominguez, O.J.R., Ríos, M.E., Rivera, O., Rodríguez, N., Rojas, A., Särkinen, T.,

Sánchez, R., Smith, M., Vargas, C., Villanueva, B., Pennington, R.T., 2016. Plant diversity patterns in neotropical dry forests and their conservation implications. Science 353, 1383–1387.
Brando, P.M., Balch, J.K., Nepstad, D.C., Morton, D.C., Putz, F.E., Coe, M.T., Silvério, D., Macedo, M.N., Davidson, E.A., Nóbrega, C.C., Alencar, A., Soares-Filho, B.S., 2014. Abrupt increases in Amazonian tree mortality due to drought–fire interactions. In: Proceedings of the National Academy of Sciences.
Chaplin-Kramer, R., Ramler, I., Sharp, R., Haddad, N.M., Gerber, J.S., West, P.C., Mandle, L., Engstrom, P., Baccini, A., Sim, S., Mueller, C., King, H., 2015. Degradation in carbon stocks near tropical forest edges. Nat. Commun. 6.
Chen, B.Q., Li, X.P., Xiao, X.M., Zhao, B., Dong, J.W., Kou, W.L., Qin, Y.W., Yang, C., Wu, Z.X., Sun, R., Lan, G.Y., Xie, G.S., 2016. Mapping tropical forests and deciduous rubber plantations in Hainan Island, China by integrating PALSAR 25-m and multi-temporal Landsat images. Int. J. Appl. Earth Obs. Geoinf. 50, 117–130.
De Sy, V., Herold, M., Achard, F., Beuchle, R., Clevers, J.G.P.W., Lindquist, E., Verchot, L., 2015. Land use patterns and related carbon losses following deforestation in South America. Environ. Res. Lett. 10.
DiMiceli, C.M., Carroll, M.L., Sohlberg, R.A., Huang, C., Hansen, M.C., Townshend, J.R.G., 2011. Annual Global Automated MODIS Vegetation Continuous Fields (MOD44B) at 250 m Spatial Resolution for Data Years Beginning Day 65, 2000–2010, Collection 5 Percent Tree Cover. University of Maryland, College Park, MD, USA.
Dong, J.W., Xiao, X.M., Sheldon, S., Biradar, C., Duong, N.D., Hazarika, M., 2012. A comparison of forest cover maps in mainland Southeast Asia from multiple sources: PALSAR, MERIS, MODIS and FRA. Remote Sens. Environ. 127, 60–73.
Dong, J.W., Xiao, X.M., Chen, B.Q., Torbick, N., Jin, C., Zhang, G.L., Biradar, C., 2013. Mapping deciduous rubber plantations through integration of PALSAR and multi-temporal Landsat imagery. Remote Sens. Environ. 134, 392–402.
Espirito-Santo, F.D.B., Keller, M., Braswell, B., Nelson, B.W., Frolking, S., Vicente, G., 2010. Storm intensity and old-growth forest disturbances in the Amazon region. Geophys. Res. Lett. 37.
European Space Agency, 2016. Land Cover CCI Product User Guide (Version 2).
Fanin, T., van der Werf, G.R., 2015. Relationships between burned area, forest cover loss, and land cover change in the Brazilian Amazon based on satellite data. Biogeosciences 12, 6033–6043.
Food and Agriculture Organization of the United Nations, 2012. Global Forest Resource Assessment (FRA) 2010. FAO, Rome, Italy.
Fraser, B., 2014. Deforestation: carving up the Amazon. In: Nature, News Feature.
Friedl, M.A., Sulla-Menashe, D., Tan, B., Schneider, A., Ramankutty, N., Sibley, A., Huang, X.M., 2010. MODIS collection 5 global land cover: algorithm refinements and characterization of new datasets. Remote Sens. Environ. 114, 168–182.
Giri, C., Long, J., 2014. Land cover characterization and mapping of South America for the year 2010 using Landsat 30 m satellite data. Remote Sens. 6, 9494–9510.
Haddad, N.M., Brudvig, L.A., Clobert, J., Davies, K.F., Gonzalez, A., Holt, R.D., Lovejoy, T.E., Sexton, J.O., Austin, M.P., Collins, C.D., Cook, W.M., Damschen, E.I., Ewers, R.M., Foster, B.L., Jenkins, C.N., King, A.J., Laurance, W.F., Levey, D.J., Margules, C.R., Melbourne, B.A., Nicholls, A.O., Orrock, J.L., Song, D.-X., Townshend, J.R., 2015. Habitat fragmentation and its lasting impact on Earth's ecosystems. Sci. Adv. 1.
Hansen, M.C., DeFries, R.S., Townshend, J.R.G., Carroll, M., Dimiceli, C., Sohlberg, R.A., 2003. Global percent tree cover at a spatial resolution of 500 meters: first results of the MODIS vegetation continuous fields algorithm. Earth Interact. 7.
Hansen, M.C., Potapov, P.V., Moore, R., Hancher, M., Turubanova, S.A., Tyukavina, A., Thau, D., Stehman, S.V., Goetz, S.J., Loveland, T.R., Kommareddy, A., Egorov, A., Chini, L., Justice, C.O., Townshend, J.R., 2013. High-resolution global maps of 21st-century forest cover change. Science 342, 850–853.
Herold, M., Mayaux, P., Woodcock, C.E., Baccini, A., Schmullius, C., 2008. Some challenges in global land cover mapping: an assessment of agreement and accuracy in existing 1 km datasets. Remote Sens. Environ. 112, 2538–2556.
Kaptue Tchuente, A.T., Roujean, J.L., De Jong, S.M., 2011. Comparison and relative quality assessment of the GLC2000, GLOBCOVER, MODIS and ECOCLIMAP land cover data sets at the African continental scale. Int. J. Appl. Earth Obs. Geoinf. 13, 207–219.
Keenan, R.J., Reams, G.A., Achard, F., de Freitas, J.V., Grainger, A., Lindquist, E., 2015. Dynamics of global Forest area: results from the FAO global forest resources assessment 2015. For. Ecol. Manag. 352, 9–20.
Khazendar, A., Rignot, E., Larour, E., 2007. Larsen B ice shelf rheology preceding its disintegration inferred by a control method. Geophys. Res. Lett. 34, 1–6.
Kim, D.H., Sexton, J.O., Noojipady, P., Huang, C.Q., Anand, A., Channan, S., Feng, M., Townshend, J.R., 2014. Global, Landsat-based forest-cover change from 1990 to 2000. Remote Sens. Environ. 155, 178–193.
Lehmann, E.A., Caccetta, P., Lowell, K., Mitchell, A., Zhou, Z.S., Held, A., Milne, T., Tapley, I., 2015. SAR and optical remote sensing: assessment of complementarity and interoperability in the context of a large-scale operational forest monitoring system. Remote Sens. Environ. 156, 335–348.
Li, X., Gong, P., Liang, L., 2015. A 30-year (1984–2013) record of annual urban dynamics of Beijing City derived from Landsat data. Remote Sens. Environ. 166, 78–90.
Lu, D., Weng, Q., 2007. A survey of image classification methods and techniques for improving classification performance. Int. J. Remote Sens. 28, 823–870.
Lucas, R.M., Cronin, N., Lee, A., Moghaddam, M., Witte, C., Tickle, P., 2006. Empirical relationships between AIRSAR backscatter and LiDAR-derived forest biomass, queensland, Australia. Remote Sens. Environ. 100, 407–425.
le Maire, G., Dupuy, S., Nouvellon, Y., Loos, R.A., Hakarnada, R., 2014. Mapping short-rotation plantations at regional scale using MODIS time series: case of eucalypt plantations in Brazil. Remote Sens. Environ. 152, 136–149.
Malhi, Y., Roberts, J.T., Betts, R.A., Killeen, T.J., Li, W.H., Nobre, C.A., 2008. Climate change, deforestation, and the fate of the Amazon. Science 319, 169–172.
Matricardi, E.A.T., Skole, D.L., Pedlowski, M.A., Chomentowski, W., 2013. Assessment of forest disturbances by selective logging and forest fires in the Brazilian Amazon using Landsat data. Int. J. Remote Sens. 34, 1057–1086.
Morton, D.C., DeFries, R.S., Shimabukuro, Y.E., Anderson, L.O., Arai, E., Espirito-Santo, F.D.B., Freitas, R., Morisette, J., 2006. Cropland expansion changes deforestation dynamics in the southern Brazilian Amazon. Proc. Natl. Acad. Sci. U. S. A. 103, 14637–14641.
Ochoa-Quintero, J.M., Gardner, T.A., Rosa, I., Ferraz, S.F.D., Sutherland, W.J., 2015. Thresholds of species loss in Amazonian deforestation frontier landscapes. Conserv. Biol. 29, 440–451.
Olofsson, P., Stehman, S.V., Woodcock, C.E., Sulla-Menashe, D., Sibley, A.M., Newell, J.D., Friedl, M.A., Herold, M., 2012. A global land-cover validation data set, part I: fundamental design principles. Int. J. Remote Sens. 33, 5768–5788.
Olofsson, P., Foody, G.M., Herold, M., Stehman, S.V., Woodcock, C.E., Wulder, M.A., 2014. Good practices for estimating area and assessing accuracy of land change. Remote Sens. Environ. 148, 42–57.
Pan, Y.D., Birdsey, R.A., Fang, J.Y., Houghton, R., Kauppi, P.E., Kurz, W.A., Phillips, O.L., Shvidenko, A., Lewis, S.L., Canadell, J.G., Ciais, P., Jackson, R.B., Pacala, S.W., McGuire, A.D., Piao, S.L., Rautiainen, A., Sitch, S., Hayes, D., 2011. A large and persistent carbon sink in the World's forests. Science 333, 988–993.
Pengra, B., Long, J., Dahal, D., Stehman, S.V., Loveland, T.R., 2015. A global reference database from very high resolution commercial satellite data and methodology for application to Landsat derived 30 m continuous field tree cover data. Remote Sens. Environ. 165, 234–248.
Phillips, O.L., Aragao, L.E.O.C., Lewis, S.L., Fisher, J.B., Lloyd, J., Lopez-Gonzalez, G., Malhi, Y., Monteagudo, A., Peacock, J., Quesada, C.A., van der Heijden, G., Almeida, S., Amaral, I., Arroyo, L., Aymard, G., Baker, T.R., Banki, O., Blanc, L., Bonal, D., Brando, P., Chave, J., de Oliveira, A.C.A., Cardozo, N.D., Czimczik, C.I., Feldpausch, T.R., Freitas, M.A., Gloor, E., Higuchi, N., Jimenez, E., Lloyd, G., Meir, P., Mendoza, C., Morel, A., Neill, D.A., Nepstad, D., Patino, S., Penuela, M.C., Prieto, A., Ramirez, F., Schwarz, M., Silva, J., Silveira, M., Thomas, A.S., ter Steege, H., Stropp, J., Vasquez, R., Zelazowski, P., Davila, E.A., Andelman, S., Andrade, A., Chao, K.J., Erwin, T., Di Fiore, A., Honorio, E., Keeling, H., Killeen, T.J., Laurance, W.F., Cruz, A.P., Pitman, N.C.A., Vargas, P.N., Ramirez-Angulo, H., Rudas, A., Salamao, R., Silva, N., Terborgh, J., Torres-Lezama, A., 2009. Drought sensitivity of the Amazon rainforest. Science 323, 1344–1347.
Qin, Y.W., Xiao, X.M., Dong, J.W., Zhang, G.L., Shimada, M., Liu, J.Y., Li, C.G., Kou, W.L., Moore, B., 2015. Forest cover maps of China in 2010 from multiple approaches and data sources: PALSAR, Landsat, MODIS, FRA, and NFI. ISPRS J. Photogramm. Remote Sens. 109, 1–16.
Qin, Y., Xiao, X., Dong, J., Zhang, G., Roy, P.S., Joshi, P.K., Gilani, H., Murthy, M.S., Jin, C., Wang, J., Zhang, Y., Chen, B., Menarguez, M.A., Biradar, C.M., Bajgain, R., Li, X., Dai, S., Hou, Y., Xin, F., Moore 3rd, B., 2016. Mapping forests in monsoon Asia with ALOS PALSAR 50-m mosaic images and MODIS imagery in 2010. Sci Rep 6, 20880.
Qin, Y., Xiao, X., Dong, J., Chen, B., Liu, F., Zhang, G., Zhang, Y., Wang, J., Wu, X., 2017. Quantifying annual changes in built-up area in complex urban-rural landscapes from analyses of PALSAR and Landsat images. ISPRS J. Photogramm. Remote Sens. 124, 89–105.
Randerson, J.T., Chen, Y., van der Werf, G.R., Rogers, B.M., Morton, D.C., 2012. Global burned area and biomass burning emissions from small fires. J. Geophys. Res. Biogeosci. 117.
Ranson, K.J., Sun, G.Q., 1997. An evaluation of AIRSAR and SIR-C/X-SAR images for mapping northern forest attributes in Maine, USA. Remote Sens. Environ. 59, 203–222.
Ranson, K.J., Kovacs, K., Sun, G., Kharuk, V.I., 2003. Disturbance recognition in the boreal forest using radar and Landsat-7. Can. J. Remote. Sens. 29, 271–285.
Reiche, J., Verbesselt, J., Hoekman, D., Herold, M., 2015. Fusing Landsat and SAR time series to detect deforestation in the tropics. Remote Sens. Environ. 156, 276–293.
Reiche, J., Lucas, R., Mitchell, A.L., Verbesselt, J., Hoekman, D.H., Haarpaintner, J., Kellndorfer, J.M., Rosenqvist, A., Lehmann, E.A., Woodcock, C.E., Seifert, F.M., Herold, M., 2016. Combining satellite data for better tropical forest monitoring. Nat. Clim. Chang. 6, 120–122.
Rosenqvist, A., Shimada, M., Suzuki, S., Ohgushi, F., Tadono, T., Watanabe, M., Tsuzuku, K., Watanabe, T., Kamijo, S., Aoki, E., 2014. Operational performance of the ALOS global systematic acquisition strategy and observation plans for ALOS-2 PALSAR-2. Remote Sens. Environ. 155, 3–12.
Saatchi, S.S., Nelson, B., Podest, E., Holt, J., 2000. Mapping land cover types in the Amazon Basin using 1 km JERS-1 mosaic. Int. J. Remote Sens. 21, 1201–1234.
Saatchi, S.S., Harris, N.L., Brown, S., Lefsky, M., Mitchard, E.T.A., Salas, W., Zutta, B.R., Buermann, W., Lewis, S.L., Hagen, S., Petrova, S., White, L., Silman, M., Morel, A., 2011. Benchmark map of forest carbon stocks in tropical regions across three continents. Proc. Natl. Acad. Sci. U. S. A. 108, 9899–9904.
Sexton, J.O., Song, X.P., Feng, M., Noojipady, P., Anand, A., Huang, C.Q., Kim, D.H., Collins, K.M., Channan, S., DiMiceli, C., Townshend, J.R., 2013. Global, 30-m resolution continuous fields of tree cover: Landsat-based rescaling of MODIS vegetation continuous fields with lidar-based estimates of error. Int. J. Digital Earth 6, 427–448.
Sexton, J.O., Noojipady, P., Song, X.-P., Feng, M., Song, D.-X., Kim, D.-H., Anand, A., Huang, C., Channan, S., Pimm, S.L., Townshend, J.R., 2015. Conservation policy and the measurement of forests. Nat. Clim. Chang. 6, 192–196.
Shimada, M., Isoguchi, O., Tadono, T., Isono, K., 2009. PALSAR radiometric and geometric calibration. IEEE Trans. Geosci. Remote Sens. 47, 3915–3932.
Shimada, M., Itoh, T., Motooka, T., Watanabe, M., Shiraishi, T., Thapa, R., Lucas, R., 2014. New global forest/non-forest maps from ALOS PALSAR data (2007-2010). Remote Sens. Environ. 155, 13–31.
Stehman, S.V., Olofsson, P., Woodcock, C.E., Herold, M., Friedl, M.A., 2012. A global land-cover validation data set, II: augmenting a stratified sampling design to estimate accuracy by region and land-cover class. Int. J. Remote Sens. 33, 6975–6993.

Townshend, J.R.G., Carroll, M., Dimiceli, C., Sohlberg, R., Hansen, M., DeFries, R., 2011. Vegetation Continuous Fields MOD44B, 2001 Percent Tree Cover, Collection 5. University of Maryland, College Park, Maryland.

Viña, A., McConnell, W.J., Yang, H., Xu, Z., Liu, J., 2016. Effects of conservation policy on China's forest recovery. Sci. Adv. 2.

Yuan, F., Sawaya, K.E., Loeffelholz, B.C., Bauer, M.E., 2005. Land cover classification and change analysis of the twin cities (Minnesota) metropolitan area by multitemporal Landsat remote sensing. Remote Sens. Environ. 98, 317–328.

Zarin, D.J., Harris, N.L., Baccini, A., Aksenov, D., Hansen, M.C., Azevedo-Ramos, C., Azevedo, T., Margono, B.A., Alencar, A.C., Gabris, C.S., Allegretti, A., Potapov, P., Farina, M., Walker, W.S., Shevade, V.S., Loboda, T.V., Turubanova, S., Tyukavina, A., 2016. Can carbon emissions from tropical deforestation drop by 50% in 5years? Glob. Chang. Biol. 22, 1336–1347.